



Research paper

Hydrogenated amorphous carbon films with different nanostructure: A comparative study

Kaixiong Gao^{a,c,1}, Yongfu Wang^{a,1}, Xiaoli Wei^{a,b}, Li Qiang^a, Bin Zhang^{a,*}, Junyan Zhang^{a,*}

^a State Key Laboratory of Solid Lubrication, Lanzhou Institute of Chemical Physics, Chinese Academy of Sciences, Lanzhou 730000, China

^b School of Chemical Engineering, Lanzhou University of Arts and Science, Lanzhou 730000, China

^c University of Chinese Academy of Sciences, Beijing 100049, China

HIGHLIGHTS

- The H content in carbon films can indicate the content of curved graphite structures.
- The FTIR is an effective method to obtain the content of sp^2 carbon forms.
- Quantitative analysis of nanostructures enriches the understanding of carbon films.

ARTICLE INFO

Keywords:

Nanostructure

Hydrogenated amorphous carbon film

a-C:H

FTIR

Raman

ABSTRACT

The introduction of curved graphite fragments into hydrogenated amorphous carbon films has been studied, and their contents are always estimated by TEM and Raman. Here, we detailedly discussed the advantage and disadvantage of TEM and Raman fit method. Combined with FTIR results, we clarified the chemical structures of the structural films and the bonded sites of doped H. The curved graphite structures included hexahydric carbon rings, and amorphous carbon (a-C) structures had rich olefinic groups and H. Finally, the differences among TEM, Raman, FTIR and H analysis in terms of the contents of curved graphite fragments were discussed.

1. Introduction

Although hydrogenated amorphous carbon (a-C:H) films have remarkably tribological and mechanical properties, they exhibit inherent brittleness and environment sensitivity that greatly limits their wear life in many situations [1,2]. To overcome these drawbacks, the main attention is focused on introducing some sp^2 carbon forms into a-C:H films, such as curved graphene [3–6] and graphene films [1], as a structural variable. For example, Chen et al report a facile approach for incorporating graphene nanoclusters into a-C:H films to bestow super-long wear life in vacuum environment [1]. The introduction of rolled-up and curved graphene sheets, which are the basic structural elements in fullerenes and nanotubes, can extend the inert or vacuum ultra-low friction behaviors of a-C:H films in the open or humid air, to make further applications in engineering practice [3,7]. Generally, the content of sp^2 carbon forms in a-C:H films is estimated by the intensity ratio of D peak (at 1360 cm^{-1}) and G peak (at 1560 cm^{-1}) obtained by using Raman spectroscopy which is used to probe the sp^2/sp^3 fraction and sp^2 cluster's diameter [8]. In the Chen's case, the D peak and G peak are

clearly separated due to the presence of nanographite. But the two peaks are obtained in the later case overlap in one bulging peak (owing to the topological disorders from the highly frequently cross-linkings and curvature), and the simple two symmetric-line fits are not suitable to fit Raman spectra [9–11]. Thus, it is very necessary to estimate the content of sp^2 carbon forms by combining with other methods, such as Transmission Electron Microscopy (TEM), FTIR (Reflection Fourier-transform infrared) and H analysis.

In this study, we compared the content estimation methods such as TEM, Raman, FTIR and H analysis based on nanostructural bonding configurations within a-C:H films. The configurations, proved by TEM, Raman and FTIR analyses, were curved hexahydric graphite rings embedded in a-C network which had rich olefinic groups and H. We thus proposed the ratio of aromatic rings and olefinic groups, and H content as the indications of the content of curved graphite structures. According to the results, H analysis is an indication of sp^2 -rich clusters because H atoms are distributed at the edge of the clusters. Raman fit results are obtained based on the configurations of five- six-(aromatic rings) and seven-carbon rings; FTIR results are from the unsaturated

* Corresponding authors.

E-mail addresses: bzhang@licp.cas.cn (B. Zhang), zhangjunyan@licp.cas.cn (J. Zhang).

¹ These authors contributed equally to this work.

carbon bonds in aromatic rings and olefinic chains. Because the curved graphite structures aren't observed more than the H value of ~30 at.% and Raman fit method involves the idealized distorted ring structures ranging from 5 to 7 units with the dominating 6-membered rings. The FTIR method can be considered as an effective method to obtain the content of sp^2 carbon forms. We hope the results will enrich the understanding of sp^2 -rich carbon films and provide a way to estimate the content of sp^2 carbon.

2. Experimental details

The structural films were deposited onto Si (1 0 0) and Fe substrates at room temperature using a DC-pulsed plasma chemical-vapor deposition (PECVD) system. The deposition feedstocks were the mixed gas of methane and hydrogen with a partial pressure ratio of 1:2 and 2:1. A dc bias of -1000 V was applied to the substrate holder for the films. The samples were obtained at different deposition times of 2 h, 4 h and 6 h, and called as dc 1:2 (2 h, 4 h or 6 h) and dc 2:1 (2 h, 4 h or 6 h). Prior to the deposition, the chamber was pumped down to 10^{-4} Pa. The substrate temperature heated by plasma bombardment did not exceed 120°C . The a-C:H films on Si substrates and Fe substrates were produced using the same PECVD system (CH_4 30 SCCM, gas pressure 27 Pa and bias voltage 500 V). The structures of as-deposited films were revealed by high resolution transmission electron microscopy (HRTEM, FEI Tecani F30), X-ray photoelectron spectroscopy (XPS, ESCALAB 250Xi), Raman spectra (Jobin-Yvon HR-800) and Fourier transform infrared spectra (FTIR, Nexus 870). The H content was obtained in the elastic recoil detection (ERD) method [7]. The cross-section of the film was measured by field emission scanning electron microscope (FESEM, JEOL JSM-6701F).

The plan-view TEM samples for observation were first deposited on the NaCl single crystal substrate and then followed by dissolution of the NaCl substrate with deionized water; the freed fragments of the films were last placed onto Cu grids to conduct observations. The samples were cut to size 10×10 mm, and the quantities of hydrogen in the samples could be measured by ERD method using a 2.04 MeV He^+ beam. The XPS was operating with Al-K α radiation and detecting chamber pressure of below 10^{-6} Pa, and the Au thin films about 0.2 nm thick were deposited on the tested carbon film surfaces to minimize the charging effect in the XPS analysis. The samples were detected in Raman spectrometer with a power below 0.5 MW m^{-2} (can avoid their unintentional damage). The FTIR spectra of the films were obtained using a Harrick Scientific horizontal reflection Ge-attenuated total reflection accessory (GATR, 65° incidence angle). To eliminate the effect of H_2O and CO_2 , the pressure in sample chamber and optical chamber was kept below 6.0×10^{-4} MPa. The spectra were collected for 64 scans with a resolution of 4 cm^{-1} .

3. Results and discussion

3.1. TEM analysis

Ordered domains of several nanometers in size consists of curved graphene sheets, as compared with that of a-C:H film (Fig. 1a). The layer spacing is approximately 0.34 nm. With increasing the CH_4/H_2 ratio, the dc 1:2 sample visually has fewer graphene layers and larger area of a-C structures than the dc 2:1 sample. In addition, the SEAD image at dc 2:1 sample shows the innermost sharper ring with lattice spacing of 3.5 \AA (matches the plane separation of hexagonal basal planes of graphite (0 0 2)), compared to the a-C:H film (top right corner of Fig. 1a and b). The quantitative estimation of curved graphene structures by visual inspection has been used in the studies [12,13]. But the TEM work has its own shortcomings, owing to the possible structural damage by the electron beam, the near surface regions of 1 nm or so may have already been altered [14,15].

3.2. Raman analysis

Pentagons and heptagons are formed in hexahydric graphite structures, resulting in the formation of curved graphene structures. In other word, the observedly curved and curled sheets in Fig. 1(b) and (c) confirm the presence of fullerene-like elements, in which both of the pentagons and heptagons are distributed randomly throughout a hexagonal network. The evidence for the odd rings can be always obtained using the Raman fit model, which involves four vibrational bands, $5A_{1g}$ at 1470 cm^{-1} (from five C-atom rings), and $7A_{1g}$ at 1200 cm^{-1} (from seven C-atom rings), $6A_{1g}$ at 1360 cm^{-1} and $6E_{2g}$ at 1560 cm^{-1} (from six C-atom rings) (Fig. 2(a)) [7,9]. The fit method has a good fitting quality, compared to the fitting of a-C:H film's spectroscopy into simple two symmetric-line fits at 1360 (*D*-mode) and 1560 cm^{-1} (*G*-mode) (Fig. 2(b)) [16].

The two structural films have some unusual peaks at 700 , 860 and 1200 cm^{-1} , which disappeared in their spectra (Fig. 3(a) and (b)). The peaks at about 700 and 1200 cm^{-1} have been assigned to fullerene-like or onion-like structures, but the assignment of the sharp band near 860 cm^{-1} is controversial because of the underlying Si substrates. He et al. [17] and Veres et al. [18] observed the band from incorporated Si and hydrogenated amorphous carbon (a-C:H:Si) films and argued that it should be related to the amorphous SiC transition layer between the films and Si substrates. The peak also was observed from the hydrogenated carbon films (a-C:H), which had 670 nm thick and 50 nm SiC transition layer deposited at Si wafers [19]. Recently, we found that the peak near 860 cm^{-1} would appear in the Raman spectra from the related wear track, after the Al_2O_3 balls slid on the fullerene-like a-C:H films with underlying Si substrates about 30 min [12]. But Roy et al. studied in detail the Raman spectra of pure carbon nano-onions, which had three low/intermediate wave number bands near 400 , 700 and 860 cm^{-1} , and they explained that the relaxation of the Raman selection rule, due to the curvature of the graphene planes in the shells, was presumed to be the cause of the appearance of the bands [20]. Similar band about 860 cm^{-1} was also appeared in the Raman spectra acquired from multishell nanographite and single wall carbon nanotubes, and could be assigned to the phonon near the point of the Brillouin zone due to the graphene plane curvature [21–23]. Therefore, regarding the assignment of the peak near 860 cm^{-1} , the further information is obtained from Fig. 3(b). Fig. 3(b) shows the Raman spectroscopy of the hydrogenated carbon films on Fe substrates. The films has a same deposition condition with the dc 2:1 films on Si substrates, as shown in the experiments above. These peaks at about 700 and 1200 cm^{-1} characteristic of curved graphene structures can be not only seen, but the peak near 860 cm^{-1} is also present in the Raman spectrum from the Fe substrates. The 860 cm^{-1} peak can therefore be attributed to the curved graphene structures in our films.

However, Raman spectroscopy is a surface detection system with a limit of probing depth of 50 – 100 nm for visible excitation. The as-prepared film with the reactive time of 4 h has thicknesses of about 550 nm, which is beyond Raman detectability. The spectrum thereby is reflected the surface nature of the film and it is difficult to recognize bulk nature. Fig. 4(b) shows the thickness for the dc 2:1 films, and the thickness are plotted with the deposition time from 2 , 4 , to 6 h. As the reactive time increases from 2 h to 4 h, the signature of pentatomic and heptatomic rings show obvious increase. When the time increases to 6 h, the signature decreases. The content of curved graphene fragments with dominating 6-membered rings, has a oppose tendency with the signature of the odd rings, which indicates that the content of curved graphene fragments isn't invariable in reactive time. Thus, Raman spectroscopy isn't an effective detection for obtaining bulk nature for carbon films.

In summary, we can obtain the content of curved graphene in carbon films' surface by Raman analysis based on the features: (1) the presence of 700 , 860 and 1200 cm^{-1} ; (2) the fit method involving the physical characteristics of idealized five-, six-, and seven-membered π -

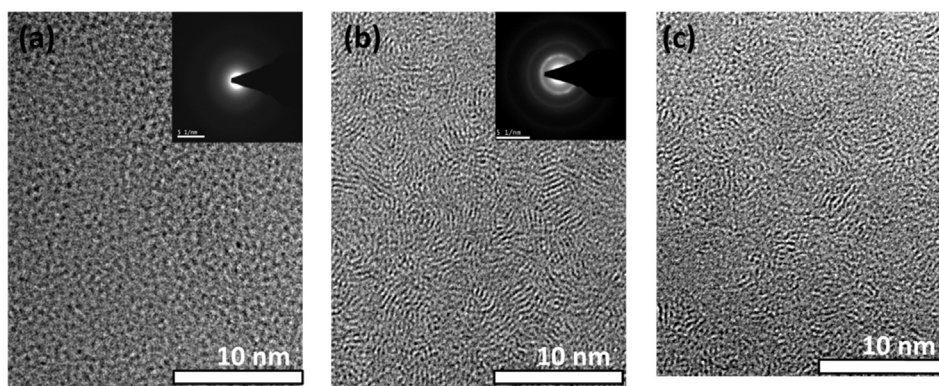


Fig. 1. Plan-view HRTEM image of a-C:H (a), the samples of dc 2:1 (b) and dc 1:2 (c) with curved graphene structures.

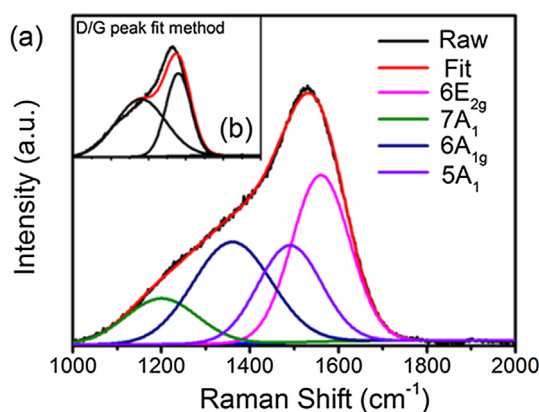


Fig. 2. Raman spectra of dc 2:1 sample with curved graphene structures. The spectrum is deconvoluted into four Gaussian peaks at about 1200, 1360, 1470, and 1560 cm^{-1} (a) or two Gaussian peaks at 1360 cm^{-1} (D-band) and 1560 cm^{-1} (G-band) (b).

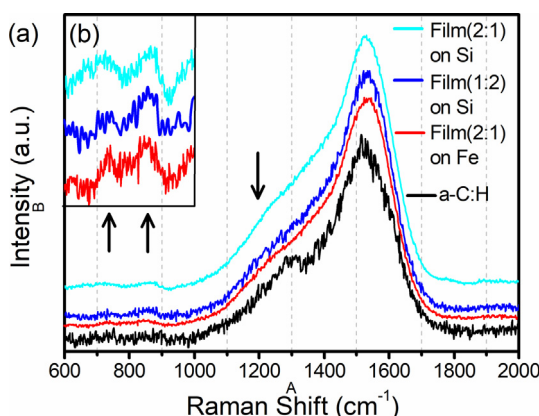


Fig. 3. Raman spectra (a) of a-C:H film, the samples of dc 2:1 and dc 1:2 with curved graphene structures on Si substrates, and dc 2:1 sample on Fe substrates. (b) Magnified wave number region from 600 to 1000 cm^{-1} in the Raman spectra of (a).

bonded carbon rings [24]. Based on the sensitive to surface structural changes, Raman spectroscopy is an appropriate probe to reveal the structure-performance relationship for the nanostructural a-C:H films, which are deposited on the condition of different parameters such as gas partial pressure, negative substrate bias, supply power, substrates, or deposition time and so on.

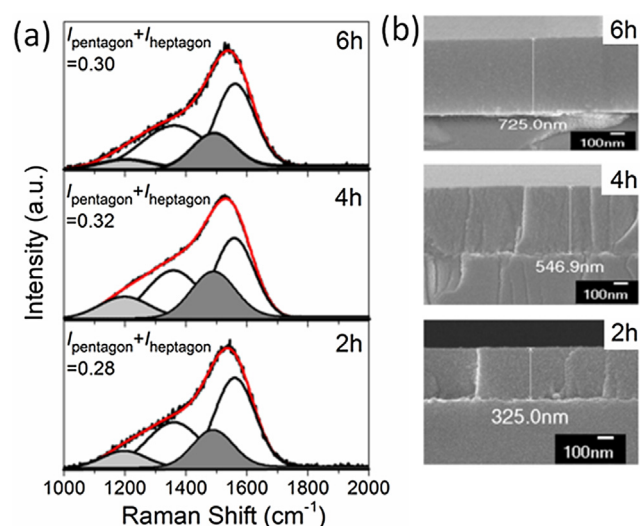


Fig. 4. Raman spectra of dc 2:1 sample on Si substrates with reactive time of 2 h, 4 h and 6 h. (b) the thickness of corresponding films in (a).

3.3. FTIR analysis

Curved graphene fragments are introduced into a-C:H films, and the films are referred as graphite-like, fullerene-like, and embedded graphene (if the long range order graphitic structure is pronounced), in terms of the size and curvature of the fragments. However, the internal chemical structure of the structural films is not well understood. According to our TEM and SEAD results, the films can be considered as a nanocomposite thin film with curved hexahydric graphite fragments (include dominant aromatic rings) embedded in a-C network. Corresponding XPS measures show the C1s positions of the films are close to that of graphite, providing evidences for the possible presence of curved graphene sheets (Fig. 5(b)). Moreover, the XPS results also indicate that a-C structures can be inferred to contain considerable fractions of sp^2 -like carbon, and thus a-C structures have rich olefinic groups. In order to get a better understanding, the reflection FTIR spectra are invoked to determine the configurations. The samples have dominant aromatic rings and/or olefinic chain, for there is a strong absorption peak centered at 1600 cm^{-1} (Fig. 5(a)). For pure carbon films, there are two peaks at 1580 and 1640 cm^{-1} (Fig. 6(a)), which respectively comes from sp^2 -hybridized carbons in aromatic rings and olefinic chain [25,26]. Therefore, FTIR results can be used to measure sp^2 carbon content, and considered as an indication of the ratio of curved graphite and a-C structures, which is measured by the intensity ratio of aromatic ring clusters/olefinic groups.

Based on the chemical structure above, we subtract a straight line formed with two maximum points on the two sides of $\sim 1600 \text{ cm}^{-1}$

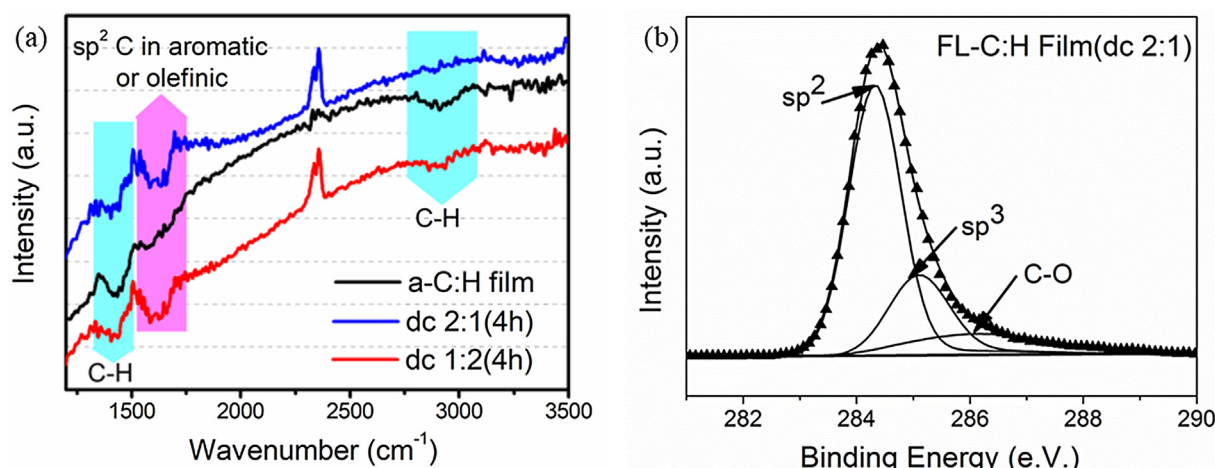


Fig. 5. FTIR spectra of a-C:H, the samples of dc 2:1 and dc 1:2 with curved graphene structures (a) and XPS of the samples of dc 2:1 (b).

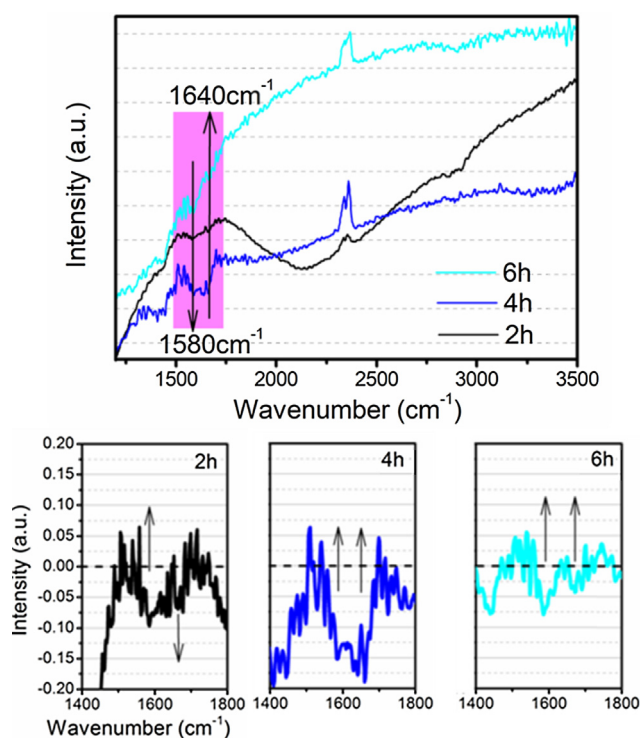


Fig. 6. (a) FTIR spectra of the dc 2:1 sample on Si substrates with reactive time of 2 h, 4 h and 6 h. (b) Subtracted spectra of corresponding films in (a).

peak for the dc 2:1 sample prepared with different reactive time, as shown in Fig. 6(b). The two peaks at 1580 and 1640 cm^{-1} can be seen clearly. The ratio of aromatic ring clusters (A) and olefinic groups (O) first decreases, and then increases with the reactive time. The content of aromatic rings is obtained by $I_A/I_A + I_O$. Because aromatic rings dominantly exist in curved graphene structures, the content of curved graphene structures is ~ 0.56 , ~ 0.43 and ~ 0.60 , respectively, corresponded to the reactive time of 2 h, 4 h and 6 h. As compared with the Raman results that the fractions of 6-membered rings are 0.72, 0.68 and 0.70 (Fig. 4), the FTIR results are lower than those by Raman. The difference may be due to the shortcomings of the Raman fit method, based on idealized ring structures involving five-, six-, and seven-membered π -bonded carbon rings which are unlikely to occur in the real films. Nevertheless, the change tendency of the content measured by FTIR and Raman is consistent.

The aromatic ring content is inversely proportional to the content of

olefinic groups (Fig. 6b). Thus, the films at 4 h have least aromatic rings, most pentagons and heptagons and most olefinic groups, which means the topological disorders are progressively introduced into the hexahydric graphene layers, and the layers become smaller and more disordered [16,27]. At this stage, the films may include more fullerene-like elements and less graphite-like features, and its layers develop more curvature and cross-link. Conversely, the films at 2 h and 6 h have a graphite-like character because high content aromatic ring clusters grow in size to form layered graphite structures.

3.4. H Analysis

However, the bonded sites of the doped H are unknown, or not involved after curved graphene fragments are introduced into a-C:H films in previous studies. In Fig. 5, a phenomenon can't be ignored that the intensity of C–H absorption peak at 1450 and 2890 cm^{-1} [26,28] markedly weaken in the dc 2:1 and dc 1:2 samples compared to that of the a-C:H films. Moreover, the dc 2:1 sample has the weaker intensity of C–H absorption than that of dc 1:2 sample, which has a high CH_4/H_2 ratio. It is thus inferred that lower hydrogen surrounding in the samples results from the production of aromatic rings and/or olefinic chain. Where are the bonded sites of the doped H? From the Section 3.3, curved graphene structures include hexahydric graphite rings, and a-C structures have rich olefinic groups. The graphite rings' sheet creation looks more reasonable than the olefinic groups, which can significantly cause the decrease of H as in the samples (Fig. 7). Based on these, H is preferentially present in a-C structures that have rich olefinic groups, and the film only have two components: H-rich a-C and curved graphene structures. Moreover, according to our results from TEM, SEAD, XPS and FTIR results, the films can be considered as a nanocomposite thin film with curved hexahydric graphite fragments (include dominant

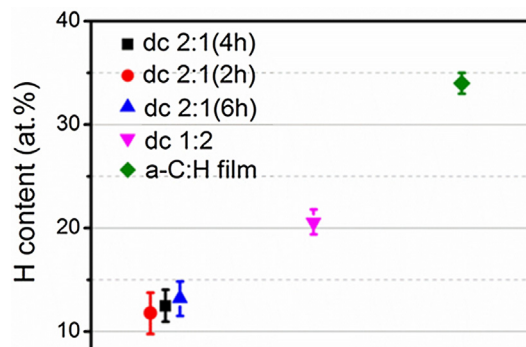


Fig. 7. Hydrogen content analysis in different films.

aromatic rings) embedded in a-C network (which had rich olefinic groups and H). Thus, H analysis is an indication of sp^2 -rich clusters because H atoms are distributed at the edge of the clusters. But the method involving H analysis is limited as follows: (1) it can hardly be taken to be a guarantee that every distributed a-C structures' sites shall have enough H; (2) the curved graphene structures have been only observed when the hydrogen content does not exceed 30 at.% in a-C:H films.

4. Conclusion

In summary, we have discussed the advantage and disadvantage of the TEM, Raman, FTIR and H analysis that had used to measure the content of curved graphite fragments in a-C:H films. Based on the configurations including curved hexahydric graphite rings embedded in a-C network which has rich olefinic groups and H, FTIR method can be considered as an effective method to obtain the content of sp^2 carbon forms. We expect that the preceding discussions will enrich the understanding of the detections measuring the content of curved graphite fragments in nanostructural films.

Acknowledgments

This work is supported by the National Natural Science Foundation of China (No. 51475447, 51661135022, 51611530704), Natural Science Foundation of Gansu Province (Grant No. 18JR3RA233), Foundation of Lanzhou University of Arts and Science (No. 2017XJZZ07) and Youth Innovation Promotion Association CAS (2017459).

References

[1] H. Song, L. Ji, H. Li, X. Liu, W. Wang, H. Zhou, J. Chen, *ACS Appl. Mater. Interfaces*

- 8 (2016) 6639.
 [2] C. Wang, S. Yang, Q. Wang, Z. Wang, J. Zhang, *Nanotechnology* 19 (2008) 225709.
 [3] Y. Wang, K. Gao, J. Zhang, *J. Appl. Phys.* 120 (2016) 045303.
 [4] C. Wang, D. Diao, X. Fan, C. Chen, *Appl. Phys. Lett.* 100 (2012) 231909.
 [5] C. Goyenola, G.K. Gueorguiev, S. Stafström, L. Hultman, *Chem. Phys. Lett.* 506 (2011) 86.
 [6] G.K. Gueorguiev, J. Neidhardt, S. Stafström, L. Hultman, *Chem. Phys. Lett.* 401 (2005) 288.
 [7] Y. Wang, K. Gao, B. Zhang, Q. Wang, J. Zhang, *Carbon* 137 (2018) 49.
 [8] A.C. Ferrari, J. Robertson, *Phys. Rev. B* 64 (2001) 075414.
 [9] M. Lejeune, M. Benlahsen, R. Bouzerar, *Appl. Phys. Lett.* 84 (2004) 344.
 [10] Jin-Koog Shin, Churl Seung Lee, Kwang-Ryeol Lee, Kwang Yong Eun, *Appl. Phys. Lett.* 78 (2001) 631.
 [11] M.P. Siegal, D.R. Tallant, L.J. Martinez-Miranda, J.C. Barbour, R.L. Simpson, D.L. Overmyer, *Phys. Rev. B* 61 (2000) 10451.
 [12] Y. Wang, J. Guo, K. Gao, B. Zhang, A. Liang, J. Zhang, *Carbon* 77 (2014) 518.
 [13] J. Zhao, Y. He, Y. Wang, W. Wang, L. Yan, J. Luo, *Tribol. Int.* 97 (2016) 14.
 [14] S. Liu, C. Zhang, E. Osman, X. Chen, T. Ma, Y. Hu, J. Luo, E. Ali, *Sci. China Technol. Sci.* 59 (2016) 1795.
 [15] T. Polcar, F. Gustavsson, T. Thersleff, S. Jacobson, A. Cavaleiro, *Faraday Discuss.* 156 (2012) 383.
 [16] A.C. Ferrari, J. Robertson, *Phys. Rev. B* 61 (2000) 14095.
 [17] X.M. He, K.C. Walter, M. Nastasi, S.T. Lee, M.K. Fung, *J. Vac. Sci. Technol. A* 18 (2000) 2143.
 [18] M. Veres, M. Koós, S. Tóth, M. Füle, I. Pócsik, A. Tóth, M. Mohai, I. Bertóti, *Diamond. Relat. Mater.* 14 (2005) 1051.
 [19] L. Cui, Z. Lu, L. Wang, *Carbon* 66 (2014) 259.
 [20] D. Roy, M. Chhowalla, H. Wang, N. Sano, I. Alexandrou, T.W. Clyne, G.A.J. Amaratunga, *Chem. Phys. Lett.* 373 (2003) 52.
 [21] R. Saito, A. Jorio, A.G. Souza Filho, A. Grueneis, M.A. Pimenta, G. Dresselhaus, M.S. Dresselhaus, *Physica B* 323 (2002) 100.
 [22] V.Y. Osipov, A.V. Baranov, V.A. Ermakov, T.L. Makarova, L.F. Chungong, A.I. Shames, K. Takai, T. Enoki, Y. Kaburagi, M. Endo, A.Y. Vul, *Diamond. Relat. Mater.* 20 (2011) 205.
 [23] K. Bogdanov, A. Fedorov, V. Osipov, T. Enoki, K. Takai, T. Hayashi, V. Ermakov, S. Moshkalev, A. Baranov, *Carbon* 73 (2014) 78.
 [24] T. Doyle, J. Dennison, *Phys. Rev. B* 51 (1995) 196.
 [25] J. Robertson, *Mat. Sci. Eng. R* 37 (2002) 129.
 [26] Y. Wang, K. Gao, Q. Wang, J. Zhang, *Chem. Phys. Lett.* 692 (2018) 258.
 [27] Y. Wang, K. Gao, J. Zhang, *Appl. Surf. Sci.* 439 (2018) 1152.
 [28] Y. Wang, K. Gao, J. Shi, J. Zhang, *Chem. Phys. Lett.* 660 (2016) 160.